Journal of Applied Polymer Science

Electrical Properties of Sorbitol-Doped Poly(vinyl alcohol)–Poly(acrylamide-*co*-acrylic acid) Polymer Membranes

Vinitha Josh,[1] Mohammad Y. Haik,[2] Ahmad I. Ayesh,[1] Mahmoud A. Mohsin,[3] Yousef Haik[2,4]

[1]Department of Physics, United Arab Emirates University, Al Ain, United Arab Emirates

[2]Department of Mechanical Engineering, United Arab Emirates University, Al Ain, United Arab Emirates

[3]Department of Chemistry, University of Sharjah, Sharjah, United Arab Emirates

[4]Center for Research Excellence in Nanobiosciences, University of North Carolina at Greensboro, Greensboro, North Carolina

Correspondence to: A. I. Ayesh (E-mail: ayesh@uaeu.ac.ae)

ABSTRACT: Solid polymer membranes from poly(vinyl alcohol) (PVA) and poly(acrylamide-*co*-acrylic acid) (PAA) with varying doping ratios of sorbitol were prepared using the solution casting method. The films were examined with Fourier transform infrared spectroscopy, thermogravimetric analysis, differential scanning calorimetry, and AC impedance spectroscopy. The impedance measurements showed that the ionic conductivity of PVA–PAA polymer membrane can be controlled by controlled doping of sorbitol within the polymer blends. The PVA–PAA–sorbitol membranes were found to exhibit excellent thermal properties and were stable for a wide temperature range (398–563K), which creates a possibility of using them as suitable polymers for device applications. © 2012 Wiley Periodicals, Inc. J. Appl. Polym. Sci. 128: 3861–3869, 2013

KEYWORDS: composites; conducting polymers; plasticizer; properties and characterization

Received 19 June 2012; accepted 19 September 2012; published online 12 October 2012
DOI: 10.1002/app.38619

INTRODUCTION

The interest in solid materials with ionic conduction properties has increased during the last 20 years owing to their application in solid-state batteries and electrochromic devices.[1,2] Much attention has been focused on investigating polymer films to enhance their mechanical properties and ambient temperature conductivity by blending various polymers,[3–5] crosslinking,[6] insertion of ceramic filters,[7] plasticization,[8] and so on. Among the various methods of producing high ionic conduction, polymer blend is a valid and feasible approach.[9,10] In agreement with Wieczorek and coworkers,[11,12] the addition of particles (fillers) produces changes in the vitreous transition temperature that alternate the temperature dependence of crystallization and in the ionic conduction of the material.

Poly(vinyl alcohol) (PVA) is a polymer which has been investigated by many researchers because of its applications as binder, and excellent biocompatibility for double-layer capacitors and electrochemical stability.[13,14] It contains carbon chain backbone with hydroxyl groups attached to methane carbons. The OH groups can be a source of hydrogen bonding and hence the assistance in the formation of polymer blends.[15] The conductivity of PVA polymer films increases noticeably by blending PVA with other suitable polymers. Poly(acrylamide-*co*-acrylic acid) (PAA) has a wide range of applications as a stabilizer and a flocculent in many technological and ecological processes. PAA finds application as a flocculent when its molecular weight is higher than 1,000,000 Da.[16] PVA and PAA are hydrophilic polymers that have been used in many biomedical applications as active hydrogels.[17] PAA chains can be trapped in PVA network while crosslinking and also forming new bonds.

Plasticizers used for polymer membrane films are generally of low-molecular-weight aprotic solvents having high dielectric constant, and they play an important role in the conducting matrix. Usually, plasticizers are added to rigid polymers, soften them, increase the processability, and lower their glass transition temperature (T_g). Basically, plasticizers make it easier for changes in molecular conformation to occur;[15] therefore, ionic conductivity of polymer blends can be improved by the addition of a particular plasticizer. Furthermore, sorbitol plasticizer has a favorable effect on the mechanical properties of the polymer membrane films where it was found to decrease the hardness and elastic modulus with the increase in plasticizer concentration.[18]

EXPERIMENTAL

Polymer complexes with PVA–PAA–sorbitol were prepared using the solvent casting method. This technique is preferred for

casting thin films as it reduces the energy of melting.[19] PVA with an average molecular weight of 61,000 g/mol and PAA with an average molecular weight of 5,000,000 g/mol (Aldrich) were used in this study.

PVA and PAA were dissolved separately in deionized water (100 mL) with a concentration of 5 g each in a conical flask, and the solutions were stirred and heated continuously at 363 K for several hours until they show homogeneous nature. The solutions were then mixed together to produce jelly solution. Sorbitol plasticizer was used as a dopant with weight percentages of 1, 2, 3, and 5% w/w. Each film was casted by spreading the suspension on glass plate and kept in a hot air oven at 353 K for 24 h. The resulting films were visually examined for their dryness and free standing nature. The thicknesses of the films were between 190 and 370 μm. The purpose of plasticizing the polymer membrane matrix is to reduce the local viscosity and thereby facilitating the mobile ion to move faster within the medium which in turn enhances the mobility and hence the conductivity.[20] According to Zhang et al.,[21] the miscibility of the blend system PVA–PAA is caused by strong hydrogen bonds between the COOH— and the OH— groups, and polyester is formed during the annealing procedure.

The fundamental vibrations of the polymer complexes were studied by Fourier transform infrared spectroscopy (FTIR) analysis in the range of 4000–500 cm^{-1} using a Thermo Nicolet Corp. Nexus 470 IR spectrophotometer at room temperature with a resolution of 2 cm^{-1}. Film's impedance was measured using a Solartron 1260A Impedance/Gain-Phase Analyzer in the frequency range of 1 Hz–1 MHz. The thin polymer films were sandwiched between two stainless steel electrodes that were held using spring-loaded probes. The resistivity was obtained from the bulk resistance in the complex impedance diagram. For the temperature-dependent ionic conductivity measurements, each sample was measured inside a test chamber in the temperature range between 298 and 398 K.

Thermal stability of the polymer membranes was investigated under nitrogen gas atmosphere using a Thermogravimetric Analyzer TGA (TA Instruments, Q50) containing a thermogravimetric analysis (TGA) heat exchanger system. Each sample (~5 mg) was placed inside a tube furnace, which was heated from 298 to 873 K at a rate of 10 K/min. The results were analyzed using the TA Universal Analysis 2000 software. Differential scanning calorimeter (TA Instruments, Q200) containing a cooling system was used to determine the T_g and the decomposition temperature (T_d) of the polymer blends. About 5 mg of each sample was sealed in an aluminum DSC pan and heated from 223 to 673 K at a heating rate of 10 K/min under nitrogen purge at a flow rate of 50 mL/min.

RESULTS AND DISCUSSION

FTIR Analysis

FTIR spectroscopy was used to analyze the interactions among the atoms or ions in the polymer films and confirm the polymer complex formation. The dried films of pure polymer and blends were cut into stripes and sandwiched between two NaCl disks before placing them in the spectrophotometer. The FTIR spectra of pure PVA, PAA, PVA–PAA, and PVA–PAA–sorbitol complexes of various sorbitol compositions are shown in Figure 1(a–g). It is assumed that a crosslinking of completely miscible blend system occurs via esterification.[22] In Figure 1(a), the vibrational bands observed at 1375, 2865, and 2923 cm^{-1} are ascribed to CH_3 asymmetric stretching, symmetric stretching, and symmetric bending vibrations of pure PVA, respectively.[23] The most characteristic band for PVA is located at wave numbers larger than 3000 cm^{-1} and it belongs to the OH group. The position of C=O band at about 1711 cm^{-1} and wide band observed at 2300–3600 cm^{-1} shown in Figure 1(b) indicates that the carboxylic acid groups form dimmers. There is no absorption of PVA in the C=O region of interest.[22]

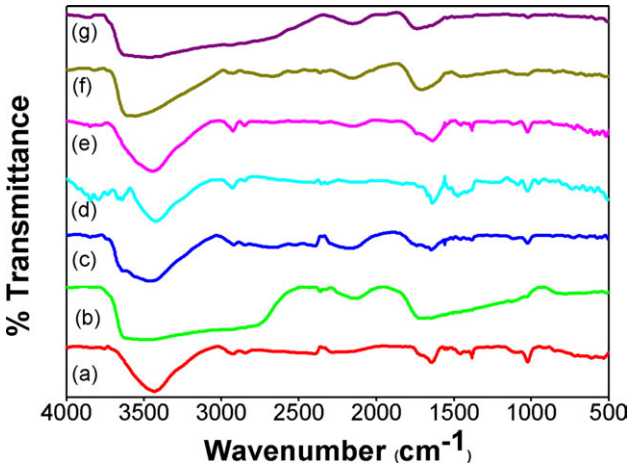

Figure 1. FTIR spectra of (a) pure PVA, (b) pure PAA, (c) pure PVA–PAA, (d) PVA–PAA–1% sorbitol, (e) PVA–PAA–2% sorbitol, (f) PVA–PAA–3 % sorbitol, and (g) PVA–PAA–5% sorbitol. [Color figure can be viewed in the online issue, which is available at wileyonlinelibrary.com.]

The peaks between 1550 and 1720 cm^{-1} shown in Figure 1(a–g) are owing to the stretching of C—O group. It can be clearly observed that with the increase in sorbitol concentration the broad peak at 3500 cm^{-1} is shifted toward the higher wavelength region, owing to hydrogen interaction with hydroxyl groups, indicating the switching of hydrogen bonds. Also, peak broadening is observed in the region of 1600–1700 cm^{-1} owing to C—C stretching. The two sharp bands observed between 2850 and 3000 cm^{-1} are assigned to the alkyl stretching mode (νCH). It is observed that as the sorbitol ratio increases, these two bands are reduced and almost disappear in the sample contacting 5% sorbitol (Figure 1(g)). However, this is not owing to the addition of sorbitol, but instead it is owing to the broadening and increased intensity of the adjacent band, which is assigned to the formation of hydrogen bonding.

Thermogravimetric Analysis

The TGA thermographs of the polymer membranes PVA–PAA–sorbitol blends of various sorbitol composition ratios are shown in Figure 2. The aim of this study is to understand quantitatively the chemical reactions occurring during the thermal treatment of polymer blends. The weight loss (percentage) of each sample with temperature is summarized in Table I. The TGA analysis in Table I and Figure 2 shows a three-step degradation process. An initial loss of about 3–6% weight occurred at 298–

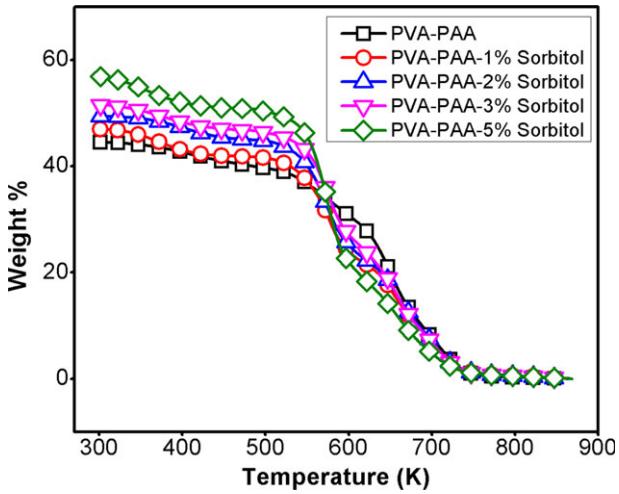

Figure 2. TGA thermographs of (a) PVA–PAA, (b) PVA–PAA–1% sorbitol, (c) PVA–PAA–2% sorbitol, (d) PVA–PAA–3% sorbitol, and (e) PVA–PAA–5% sorbitol. [Color figure can be viewed in the online issue, which is available at wileyonlinelibrary.com.]

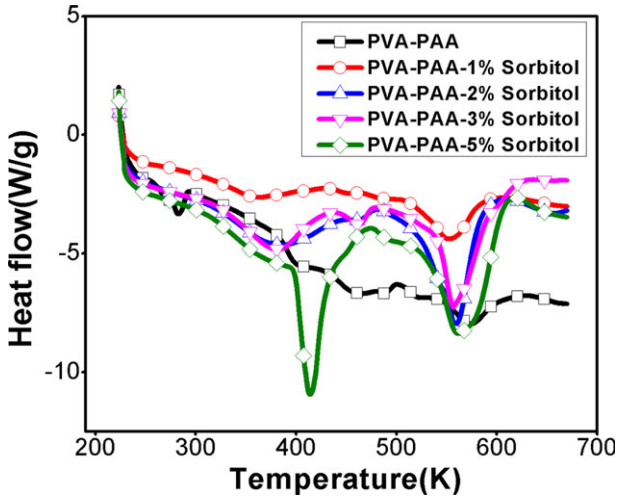

Figure 3. DSC thermographs of (a) PVA–PAA, (b) PVA–PAA–1% sorbitol, (c) PVA–PAA–2% sorbitol, (d) PVA–PAA–3% sorbitol, and (e) PVA–PAA–5% sorbitol. [Color figure can be viewed in the online issue, which is available at wileyonlinelibrary.com.]

443 K and was related to both the loss of nonbound water and the formation of intra- and intermolecular anhydrides. A second weight loss occurred in the range 513–623 K and it was associated to the decarboxylation process of intra- and intermolecular anhydrides formed during the previous dehydration and related to the dehydration of the OH groups of the copolymer.[24] Finally, the loss of weight within the range 633–773 K was related to the full degradation of the macromolecules. The decomposition of PAA occurs in the temperature range of 593–643 K and the onset decomposition temperature of PVA starts at 683 K.[22] After this temperature, the PVA–PAA–sorbitol polymer membranes become greatly degraded. It has been clearly evidenced that the PVA–PAA–sorbitol membrane samples are relatively stable in the temperature range of 373–573 K.

Differential Scanning Calorimetry

The differential scanning calorimetry (DSC) thermographs of the PVA–PAA and PVA–PAA–sorbitol polymer membrane blends of the various sorbitol composition ratios are shown in Figure 3. Transition temperature (T_g), melting temperature (T_m), and decomposition temperature (T_d) are listed in Table II. Data from Figure 3 are summarized in Table II, indicating two endothermic peaks at high temperatures. The first relaxation corresponds to the melting temperature of the solid polymer membrane films, and the second represents the decomposition temperature. A smaller peak area of T_m for the polymer membrane indicates a smaller fraction of the crystalline phase and a larger fraction of the amorphous phase which may benefit anionic transportation.[25] Owing to the addition of sorbitol, the interaction between the hydroxyl group of the sorbitol and the hydroxyl and carbonyl groups of the polymer blends increases. As the percentage of sorbitol rises, the effect of this causes the chains to be physically crosslinked via the formation of hydrogen bonding and as a consequence, the T_g subsequently increases.

Impedance Analysis

The typical temperature-dependent impedance plots (Nyquist plots) for PVA–PAA polymer membranes measured between 298 and 398 K are shown in Figure 4. Each Nyquist plot shows the dependence of the imaginary part of the impedance ($Z''(\omega)$) on the real part ($Z'(\omega)$). Herein, the total AC impedance of a material provides a quantitative measure of the induction and capacitance parts and given as: $Z(\omega) = Z'(\omega) - iZ''(\omega)$. The Nyquist plot at 298 K shows a single semicircle, whereas two semicircles appear for the plots at high temperatures. The effect of sorbitol doping on the Nyquist plots is shown in Figure 5 at 298 K. Two semicircles appear in each Nyquist plot for PVA–PAA films that are doped with sorbitol.

Table I. The Weight Loss (Percentage) of the PVA–PAA and PVA–PAA–Sorbitol Polymer Membrane at Different Temperatures by TGA Analysis

Sorbitol weight (% w/w)	Temperature region (K)		
	298–443	513–623	633–773
0	3.3	12.6	23.7
1	4.1	20.1	17
2	4.8	22.4	19.5
3	5.2	23.9	20.2
5	6	28.2	21.3

Table II. Transition Temperature (T_g), Melting Temperature (T_m), and Decomposition Temperature (T_d) of the PVA–PAA and PVA–PAA–Sorbitol Polymer Membranes with Increasing Sorbitol Weight Percentage

Sorbitol weight (% w/w)	T_g (K)	T_m (K)	T_d (K)
0	396	457	573
1	356	453	553
2	376	462	563
3	379	464	557
5	412	494	563

Applied Polymer SCIENCE

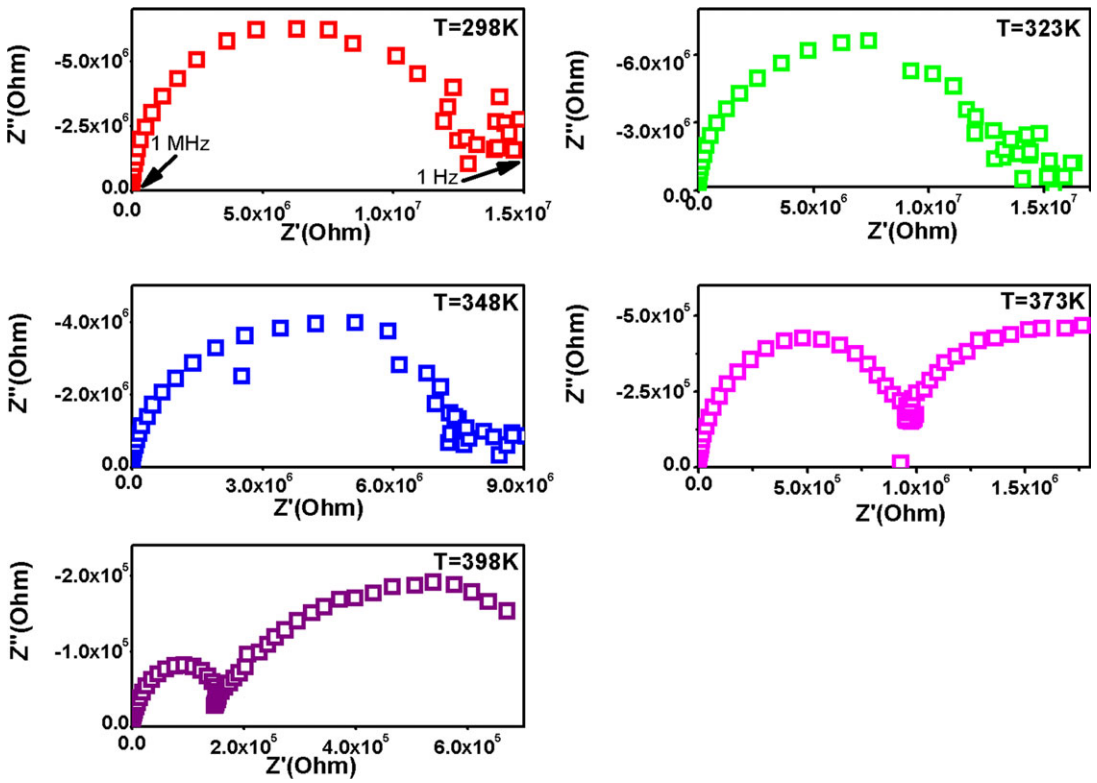

Figure 4. The impedance spectra of pure PVA–PAA with temperature variation from 298 to 398K. [Color figure can be viewed in the online issue, which is available at wileyonlinelibrary.com.]

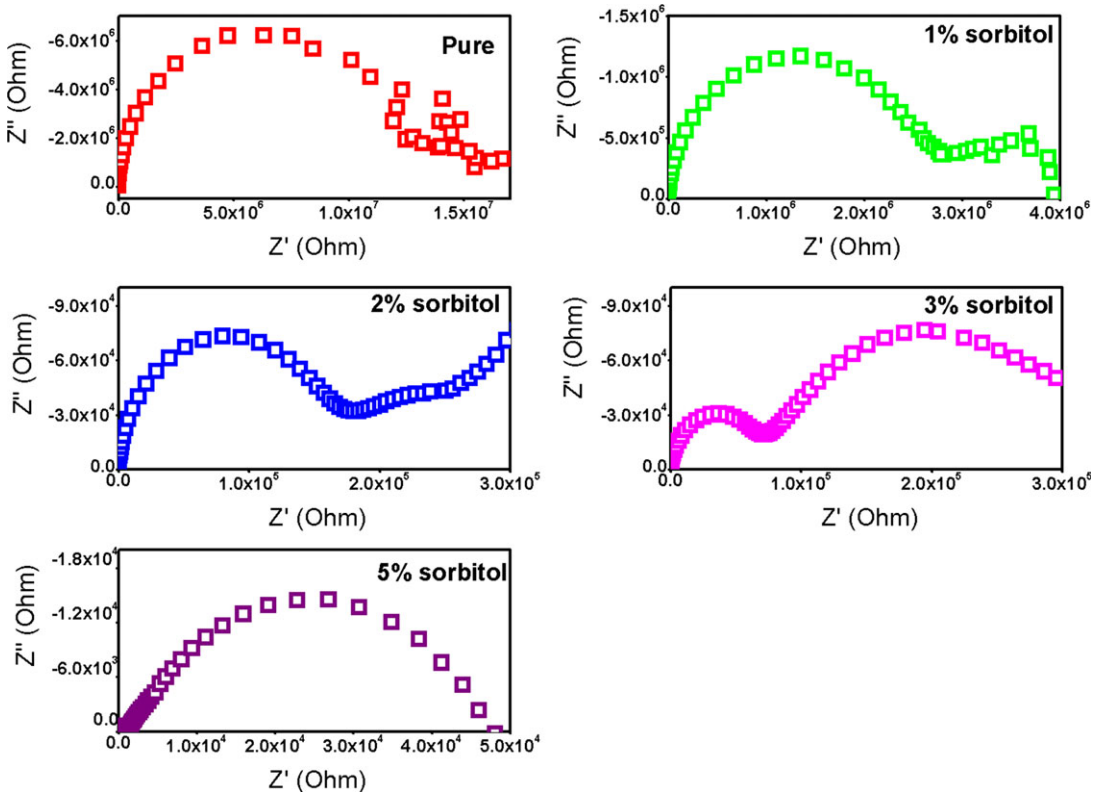

Figure 5. The dependence of the impedance spectra on the sorbitol concentration within the PVA–PAA films at 298K. [Color figure can be viewed in the online issue, which is available at wileyonlinelibrary.com.]

Table III. R_{film} and C_{film} Values for PVA–PAA and PVA–PAA–Sorbitol at Different Temperatures

	Pure mix		Mix + 1% sorbitol		Mix + 2% sorbitol		Mix + 3% sorbitol		Mix + 5% sorbitol	
T (K)	R_{film} (Ω)	C_{film} (F)	R_{film} (Ω)	C_{film} (F)	R_{film} (Ω)	C_{film} (F)	R_{film} (Ω)	C_{film} (F)	R_{film} (Ω)	C_{film} (F)
298	1.77 E + 05	3.17 E −11	2.89 E + 06	3.62 E −11	1.75 E + 05	3.94 E −11	7.87 E + 04	4.08 E −11	4.37 E + 04	4.65 E −08
323	1.39 E + 07	3.31 E −11	2.02 E + 05	4.24 E −11	1.18 E + 04	3.04 E −11	7.59 E + 03	3.30 E −11	2.01 E + 04	1.20 E −07
348	8.39 E + 06	3.75 E −11	2.15 E + 04	2.83 E −11	7.51 E + 03	1.90 E −07	1.08 E + 04	7.98 E −08	4.17 E + 03	5.09 E −07
373	9.92 E + 05	4.14 E −11	7.40 E + 03	3.45 E −11	7.84 E + 03	1.79 E −07	4.70 E + 03	1.25 E −07	8.01 E + 03	3.23 E −07
398	1.77 E + 05	4.18 E −11	3.65 E + 03	9.26 E −11						

Table IV. R_{ct} and C_{dl} Values for PVA–PAA and PVA–PAA–Sorbitol at Different Temperatures

	Pure mix		Mix + 1% sorbitol		Mix + 2% sorbitol		Mix + 3% sorbitol	
T (K)	R_{ct} (Ω)	C_{dl} (F)	R_{ct} (Ω)	C_{dl} (F)	R_{ct} (Ω)	C_{dl} (F)	R_{ct} (Ω)	C_{dl} (F)
298			1.75 E + 06	5.79 E −09	2.86 E + 05	1.23 E −08	2.80 E + 05	9.25 E −09
323			1.73 E + 05	4.37 E −09	7.11 E + 04	1.63 E −07	1.32E + 05	2.31 E −08
348			3.38 E + 04	4.68 E −08				
373	8.05 E + 05	4.00 E −08	1.37 E + 04	8.52 E −08				
398	8.02 E + 05	5.13 E −08						

Table V. The Resistivity for PVA–PAA and PVA–PAA–Sorbitol Polymer Membrane Electrodes With Temperature

	Pure mix (l = 370 μm)		Mix + 1% sorbitol (l = 210 μm)		Mix + 2% sorbitol (l = 220 μm)		Mix + 3% sorbitol (l = 200 μm)		Mix + 5%sorbitol (l = 190 μm)	
T (K)	ρ_{film} (Ω m)	ρ_{ct} (Ω m)	ρ_{film} (Ω m)	ρ_{ct} (Ω m)	ρ_{film} (Ω m)	ρ_{ct} (Ω m)	ρ_{film} (Ω m)	ρ_{ct} (Ω m)	ρ_{film} (Ω m)	ρ_{ct} (Ω m)
298	3.28 E + 05		1.32 E + 05	8.02 E + 04	7.65 E + 03	1.25 E + 04	3.78 E + 03	1.35 E + 04	2.21 E + 03	
323	3.61 E + 05		9.23 E + 03	7.93 E + 03	5.17 E + 02	3.11 E + 03	3.65 E + 02	6.32 E + 03	1.02 E + 03	
348	2.18 E + 05		9.83 E + 02	1.55 E + 03	3.28 E + 02		5.17 E + 02		2.11 E + 02	
373	2.58 E + 04	2.09 E + 04	3.39 E + 02	6.27 E + 02	3.43 E + 02		2.26 E + 02		4.06 E + 02	
398	4.61 E + 03	2.08 E + 04								

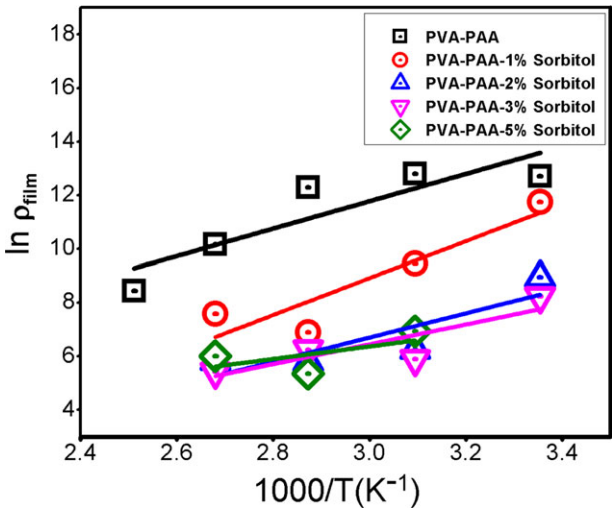

Figure 6. The inverse temperature dependence of the natural logarithm of ionic resistivity for PVA–PAA–sorbitol polymer complexes with sorbitol concentration varying from 0 to 5%. [Color figure can be viewed in the online issue, which is available at wileyonlinelibrary.com.]

The first semicircle appears in the Nyquist plots at high frequency (arrows, Figure 4), and can be simulated with an equivalent circuit of a resistance and a capacitance in parallel.[26] The resistance represents the bulk contribution to the conductivity (R_{film}) and capacitance (C_{film}) that can be associated with the dielectric relaxation of the polymer. Therefore, R_{film} and C_{film} represent the contribution to resistance and capacitance arising from the grain boundaries and electron depletion regions in the film.[27]

As shown in Figures 4 and 5, the impedance plots reveal second semicircles at low frequency with increasing temperature as well as concentration of sorbitol, indicating the double-layer response at the electrode/sample interface. Thus, each sample with two semicircles can be represented by two pairs of parallel RC circuits connected into series.[28] The low-frequency semicircles indicate the capacitive nature of the interface and the low electronic conductivity in the cell.[29] The first semicircle

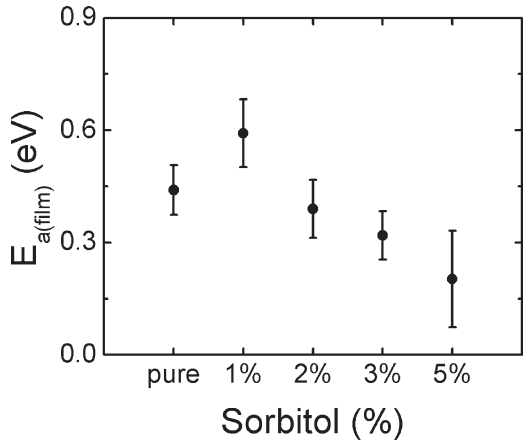

Figure 7. The variation of the film activation energy with sorbitol concentration for PVA–PAA–sorbitol polymer films.

Table VI. The Dependence of the Relaxation Time on Temperature for PVA–PAA–Sorbitol Films (With Doping Ratios of 1, 2, 3, and 5%)

	Pure mix		Mix + 1% sorbitol		Mix + 2% sorbitol		Mix + 3% sorbitol		Mix + 5% sorbitol	
T (K)	τ_{film} (s)	τ_{ct} (s)	τ_{film} (s)	τ_{ct} (s)	τ_{film} (s)	τ_{ct} (s)	τ_{film} (s)	τ_{ct} (s)	τ_{film} (s)	τ_{ct} (s)
298	3.10 E −04		1.06 E −04	1.24 E −02	1.46 E −03	6.31 E −03	1.72 E −01	3.11 E −03	1.22 E −01	
323	4.60 E −04		9.17 E −06	2.69 E −03	8.29 E −03	1.21 E −02	1.05 E −03	3.05 E −03	2.52 E −03	
348	3.15 E −04		9.52 E −07	1.60 E −03	1.43 E −03		6.13 E −04		2.12 E −03	
373	4.15 E −05		2.74 E −07	1.26 E −03	6.10 E −06		3.30 E −06		2.71 E −03	
398	7.46 E −06	5.37 E −02								

corresponds to the resistive and capacitive components (R_{film} and C_{film}) of the film and can be assigned to the ionic conduction process (kinetic process) that occurs at high frequencies. The second semicircle occurs at low frequency range and is related to the interfacial charge transfer resistance and double-layer capacitance (R_{ct} and C_{dl}); thus, it is owing to the diffusion of positive and negative charges within the polymer film.

Analysis of the Nyquist spectra yields information about the electrical characteristics of the PVA–PAA–sorbitol polymer membrane films. Herein, semicircle fittings were used to calculate the capacitances and resistances of the films which can be found from span of semicircles and the frequencies at the maxima in the Nyquist plots. The capacitance values calculated for the high-frequency semicircles vary between 10^{-11} and 10^{-7} F depending on the temperature and concentration of sorbitol as summarized in Table III. The capacitance values are typical for film relaxation phenomena, which confirm that the high-frequency semicircles represent the bulk film-response characteristic, C_{film}.[6] The low-frequency capacitances obtained at different temperatures for each concentration of sorbitol are in the range of 10^{-9}–10^{-7} F and summarized in Table IV. Table IV summarizes that the capacitance calculated for the low-frequency semicircles increases with increasing temperature for each concentration of sorbitol in the polymer films. These capacitances are related to interfacial capacitance, and can be associated with the formation of passive layers, C_{dl}.[6,30] As blocking electrodes were used in impedance analysis, each solid polymer membrane film interface can be regarded as a capacitor. When the capacitor is ideal, it should show a vertical spike in impedance diagram. However, the curvature in Figures 4 and 5 inclined at an angle (θ) of $<90^\circ$ instead of the vertical spike in the low-frequency side. This is known to be obtained from the roughness of solid polymer membrane interface.[13]

The resistance values of the film and interfacial charge transfer are listed in Tables III and IV for the PVA–PAA–sorbitol polymer membrane films. Each resistance value was converted into the resistivity (ρ) using the equation $\rho = RA/l$, where l is the thickness of the polymer film and A is the area of the blocking electrode. The calculated values of ρ_{film} and ρ_{ct} are listed in Table V.

As summarized in Table V, it is clear that as the temperature increases, the resistivity decreases, in general, for polymer films. In addition, increasing the doping concentration decreases the resistivity. This behavior is in agreement with the theory established by Armand et al..[11,31,32] This can be explained by recognizing the free volume model.[33,34] When the temperature increases, the vibrational energy of the polymer film fragment can be raised up to push against the pressure imposed by its neighboring atoms and create a small amount of space surrounding its own volume in which vibrational motion can occur.[34,35] Therefore, the increment of temperature causes the increase in conductivity owing to the increased free volume and their respective segmental mobility.[20] In addition, the free volume around the polymer chain causes the mobility of polymer blends to increase with sorbitol doping, and hence, the resistivity to decreases.

Figure 6 shows the variation of the natural logarithm of the film resistivity versus inverse temperature for PVA–PAA–sorbitol polymer films, with varying percentages of sorbitol concentration. The figure shows that the ρ_{film} decreases by increasing the doping ratio of sorbitol. It is noticeable that the slope of the curves shows a systematic decrease with the doping concentration. The results shown in Figure 6 (solid lines) are fitted into linear equations. The activation energy (E_a) of each polymer membrane film is calculated from the slopes of the curves using the Arrhenius equation[36,37]: $\rho = \rho_0 \exp(E_a/k_BT)$. Here, ρ_0 is the pre-exponential factor, T is the absolute temperature, E_a is the activation energy, and k_B is the Boltzmann constant. Figure 7 shows the dependence of the $E_{a(film)}$ on the sorbitol concentration for PVA–PAA–sorbitol polymer membrane films. Figure 7 shows that $E_{a(film)}$ decreases with increasing sorbitol concentration. It should be noted that the values of the activation energy in this study are lower than those in our earlier study[28] on PVA doped with 1-methyl-3-*n*-decylimidazolium bromide. The effect of plasticizers on the polymer segmental and conductivity depends on the specific nature of the plasticizer, including viscosity, dielectric constant, and polymer–plasticizer interaction. In this study, the plasticizer is an ionic liquid that provides more charges and decreases the viscosity of the blends by reducing the number of chain entanglements. Reducing the number of entanglements at a given ratio of plasticizer reduces the amount of orientation of macromolecular structure.[38] Therefore, the low viscosity leads to high mobility of charge carriers and thus, their segmental motion in the polymer matrices increases the conductivity.[15] Consequently, the electrical conductivity of the sorbitol plasticized films exhibit an enhancement as compared to unplasticized films.[26,36,39,40]

The relaxation times (τ_{film} and τ_{ct}) for the semicircles in Nyquist plots can be calculated using $\tau = 1/\omega_{max,}$ where ω_{max} is the angular frequency ($\omega_{max} = 2\pi f_{max}$) at the semicircle maximum.[41] The relaxation times are summarized in Table VI. It is observed from Table VI that, in general, both τ_{film} and τ_{ct} decrease with temperature. In addition, Table VI summarizes that the τ_{film} of the pure and doped films is lower than τ_{ct}. This indicates that at the high frequency range, the conductivity is dominated by the ionic conduction process in the bulk of the polymer electrode.[34,36,42] The lower value of τ_{film} than τ_{ct} is a result of the faster ionic conduction process in the polymer film than the finite length diffusion of positive and negative ions. It is clear that diffusion process occurs when an appreciable concentration of the sorbitol is present. Thus, the resistivity of the film decreases noticeably.

CONCLUSIONS

Polymer membrane films of PVA–PAA–sorbitol with varying concentration of sorbitol have been prepared by solution casting method. The polymer–sorbitol complex formation has been confirmed from FTIR spectral measurements. DSC and TGA measurements state that membranes show single T_g for all the compositions and are relatively stable in the temperature range of 273–563 K.

The conductivity of the membranes was controlled by controlling the doping level of sorbitol. It was found that both resistivities (ρ_{ct} and ρ_{film}) decrease with increasing temperature and sorbitol ratio from 1 to 5% in the PVA–PAA–sorbitol polymer complex. This is owing to the increase in the mobility and assistance of polymer segmental motion which would probably be the net effect of the decreasing viscosity on the account of higher sorbitol ratio.

REFERENCES

1. Armad, M. *Solid State Ionics* **1994,** *69*, 309.
2. Bruse, P. G. *Electro Chem. Acta* **1995,** *40*, 2077.
3. Wright, P. V. *Br. Polym. J.* **1975,** *7*, 319.
4. Quartarone, E.; Mustarelli, P.; Magistris, A. *Solid State Ionics* **1998,** *110*, 1.
5. Kim, D. W.; Park, J. R.; Rhee, H. W. *Solid State Ionics* **1996,** *83*, 49.
6. Wieckzorek, W.; Stevens, J. R. *J. Phys. Chem. B* **1997,** *101*, 1529.
7. Przyluski, J.; Wieczorek, W. *Solid State Ionics* **1989,** *36*, 165.
8. Cherng, J. Y.; Munshi, M. Z. A.; Owens, B. B.; Smyrl, W. H. *Solid State Ionics* **1988,** *28*, 857.
9. Lai, J. Y.; Chen, Y. C.; Hsu, K. Y. *J. Appl. Polym. Sci.* **1991,** *43*, 1795.
10. Varishetty, M. M.; Qiu, W.; Gao, Y.; Chen, W. *Appl. Polym. Sci.* **2010,** *50*, 878.
11. Armand, M. B.; Chabango, J. M.; Duclot, M. J. In Fast Ion Transport in Solids, Vashishta, P.; Mundy, J. N.; Shenoy, G. K.Eds., North-Holland: Amsterdam, **1979,** p 131.
12. Plocharski, J.; Wieczorek, W. *Solid State Ionics* **1998, 28–30, 979.**
13. Wu, G. M.; Lin, S. J.; Yang, C. C. *J. Membr. Sci.* **2006,** *275*, 127.
14. Fenton, D. E.; Parker, J. M.; Wright, P. V. Complexes of alkali metal ions with poly(ethylene oxide), *Polymer* **1973,** *14*, 589.
15. Rajendran, S.; Sivakumar, M.; Subadevi, R. *Mater. Lett.* **2004,** *58*, 641.
16. Grządka, E.; Chibowski, S. *Physicochem. Probl. Miner. Proc.* **2009,** *43*, 31.
17. Manavi-Tehrani, I.; Rabiee, M.; Parviz, M.; Tahriri, M. R.; Fahimi, Z. *Macromol. Symp.* **2010,** *296*, 457.
18. Mohsin, M.; Hossin, A.; Haik, Y. *Mater. Sci. Eng. A* **2011,** *528*, 925.
19. Siemann, U. *Prog. Colloid Polym. Sci.* **2005,** *130*, 1.
20. Michael, M. S.; Jacob, M. M. E.; Probaharan, S. R. S.; Radhakrishna, S. *Solid State Ionics* **1997,** *98*, 167.
21. Zhang, X.; Takegoshi, K.; Hikichi, K. *Polymer* **1992,** *33*, 718.
22. Arndt, K. F.; Richter, A.; Ludwig, S.; Zimmermann, J.; Kressler, J.; Kuckling, D.; Adler, H. *J. Acta Polym.* **1999,** *50*, 383.
23. Hema, H.; Selvasekarapandian, S.; Arunkumar, D.; Sakunthala, A.; Nithya, H. *J. Non-Cryst. Solids* **2009,** *355*, 84.
24. N.; Bertoni, F.; Ciardelli, G.; Cristallini, C.; Silvestri, D.; Coluccio, M. L.; Giusti, P. *Eur. Polym. J.* **2005,** *41*, 3004.

25. Vassal, N.; Salmon, E.; Fauvarque, J. F. *Electrochim. Acta* **2005,** *45*, 1527.
26. Amirudin, A.; Thieny, D. *Prog. Org. Coat.* **1995,** *26*, 1.
27. Varghese, O. K.; Malhothra, L. K. *J. Appl. Phys.* **2000,** *87*, 7457.
28. Ayesh, A. I.; Mohsin, M. A.; Haik, M. Y.; Haik, Y. *Curr. Appl Phys.* **2012,** *12*, 1223.
29. Huguenin, F.; Calvallcante, M. G.; Torresi, R. M. *Solid State Ionics* **1999,** *126*, 259.
30. Bruse, P. G. Polymer Electrolyte Reviews; MacCullum, J. R., Vincent, C. A., Eds.; Elsevier: London, **1987;** Vol. 1, Chapter 8.
31. Yang, C. C.; Lin, S. J.; Wu, G. M. *Mater. Chem. Phys.* **2005,** *92*, 251.
32. Andrieu, X.; Fauvarque, J. F. *Electrochim. Acta* **1995,** *40*, 2295.
33. Miyanmoto, T.; Shibayama, K. *J. Appl, Phys.* **1973,** *44*, 5372.
34. Rajendran, S.; Sivakumar, M.; Subadevi, R.; Nirmala, M. *Phys. B* **2004,** *348*, 73.
35. MacCallum, J. R.; Vincent, C. A., Eds. Polymer Electrolyte Reviews-I; Elsevier: London, **1987.**
36. Barsoukov, E.; Macdonald, J. R. Impedance Spectroscopy Theory, Experiment and Applications, 2nd ed.; Wiley-Interscience: Hoboken, NJ, **2005.**
37. Best, A. S.; Ferry, A.; MacFarlane, D. R.; Forsyth, M. *Solid State Ionics* **1999,** *126*, 269.
38. Liu, W.; Cheng, L.; Zhang, H.; Zhang, Y.; Wang, H.; Yu, M. *Int. J. Mol. Sci.* **2007,** *8*, 180.
39. Croce, F.; Appetecchi, G. B.; Slane, S.; Salomon, M.; Tavarez, M.; Arumugam, S.; Wang, Y.; Greenbaum, S. G. *Solid State Ionics* **1996,** 86–88, 307.
40. Gunot, S.; Salmon, E.; Penneau, J. F.; Fauvarque, F. *Electrochim. Acta* **1998,** *43*, 1163.
41. Fernandez, M. E.; Diosa, J. E.; Vargas, R. A. *Microelectron. J.* **2008,** *39*, 1344.
42. Venkateswarlu, M.; Narasimha Reddy, K.; Rambabu, B.; Satyanarayana, N. *Solid State Ionics* **2000,** *127*, 177.